

Efficient symmetric and asymmetric Bell-state transfers in a dissipative Jaynes-Cummings model

Qi-Cheng Wu^{1,*†}, Yu-Liang Fang^{1,*}, Yan-Hui Zhou¹, Jun-Long Zhao¹, Yi-Hao Kang², Qi-Ping Su², and Chui-Ping Yang^{2,‡}

¹*Quantum Information Research Center and Jiangxi Province Key Laboratory of Applied Optical Technology, Shangrao Normal University, Shangrao 334001, China*

²*School of Physics, Hangzhou Normal University, Hangzhou*

Symmetric or asymmetric state transfer along a path encircling an exceptional point (EP) is one of the extraordinary phenomena in non-Hermitian (NH) systems. However, the application of this property in both symmetric and asymmetric entangled state transfers, within systems experiencing multiple types of dissipation, remains to be fully explored. In this work, we demonstrate efficient symmetric and asymmetric Bell-state transfers, by modulating system parameters within a Jaynes-Cummings model and considering atomic spontaneous emission and cavity decay. The effective suppression of nonadiabatic transitions facilitates a symmetric exchange of Bell states regardless of the encircling direction. Additionally, we present a counterintuitive finding, which suggests that the presence of an EP may not be indispensable for implementation of asymmetric state transfers in NH systems. We further achieve perfect asymmetric Bell-state transfers even in the absence of an EP, while dynamically orbiting around an approximate EP. Our work presents an approach to effectively and reliably manipulate entangled states with both symmetric and asymmetric characteristics, through the dissipation engineering in NH systems.

PACS numbers: 03.67. Pp, 03.67. Mn, 03.67. HK

Keywords: Exceptional points; Adiabatic Bell-state transfer; Chiral Bell-state transfer; Jaynes-Cummings model

I. INTRODUCTION

Since the discovery of exceptional points (EPs) [1–4], a plethora of counterintuitive phenomena have emerged in non-Hermitian (NH) systems [5–8], encompassing heightened sensitivity to perturbations [9], loss-induced transparency effects [10, 11], and the existence of distinctive topological structures [12, 13]. Recent studies have also revealed that symmetric (adiabatic) state transfer [13–15] and asymmetric (chiral) state transfer [16–24] can be accomplished by adjusting system parameters along a path encircling an exceptional point (EP). In general, the symmetric switching between the eigenstates of a system implies that the state transfer is solely determined by the initial state and remains unaffected by the encircling direction. Conversely, the asymmetric switching between the system eigenstates indicates that the state transfer is solely determined by the encircling direction. The discoveries and applications of symmetric and asymmetric state transfers in time-modulated NH systems have undoubtedly made significant contributions to the advancements in the quantum field [14–16, 25–27].

However, it is unfortunate that the existing research [13–27] predominantly focuses on either symmetric or asymmetric state transfer, with a little of studies simultaneously involving both types in the same quan-

tum system. Additionally, existing state-transfer protocols still exhibit limitations primarily associated with dissipation, typically focusing on a single type such as spontaneous emission or cavity decay [14, 15, 28, 29]. The successful demonstration of symmetric or asymmetric state transfer in single-bit system is noteworthy, however, achieving efficient entangled state transfers (i.e., Bell states [30, 31]) in systems with multiple types of dissipation remains a challenging task.

In this work, we demonstrate efficient symmetric and asymmetric Bell-state transfers through modulation of system parameters in a Jaynes-Cummings (J-C) model with both atomic spontaneous emission and cavity decay. We effectively mitigate the influence of nonadiabatic transitions induced by the imaginary component of the eigenenergy spectrum through appropriate parameter configurations. Subsequently, by selecting a trajectory that dynamically encircles an EP, we successfully realize a long-desired symmetric Bell-state transfer, wherein the exchange of Bell states occurs dynamically irrespective of the encircling direction. Moreover, we present a counterintuitive finding, which suggests that the presence of an EP may not be indispensable for the successful implementation of asymmetric state transfer in NH systems. Furthermore, we achieve perfect asymmetric Bell-state transfers even in the absence of an EP, while dynamically orbiting around an approximate EP (AEP). Finally, we demonstrate that our results hold for the J-C model under time-modulated and time-independent dissipations, where the final Bell-state transfer is determined by the trajectory orientation. Our work presents a novel approach for effectively and reliably manipulating entan-

*These authors contributed equally to this work.

†E-mail: wuqi.cheng@163.com

‡E-mail: yangcp@hznu.edu.cn

gled states with both symmetric and asymmetric characteristics through the dissipation engineering in NH systems.

II. DISSIPATIVE JAYNES-CUMMINGS MODEL

We consider a dissipative Jaynes-Cummings (J-C) model, in which a two-level atom (with the ground state $|g\rangle$ and the excited state $|e\rangle$) is coupled to an optical cavity with the coupling strength g . The decay rate of the cavity mode and the atomic spontaneous emission rate are respectively indicated by κ and γ . The effective Hamiltonian describing this system can be expressed as follows [32–35] (taking $\hbar=1$)

$$H_{\text{eff}} = \omega_a a^\dagger a + \omega_e \sigma_+ \sigma_- + g(a^\dagger \sigma_- + a \sigma_+) - \frac{i\kappa}{2} a^\dagger a - \frac{i\gamma}{2} \sigma_+ \sigma_-, \quad (1)$$

where ω_a is the cavity resonance frequency, while ω_e is the transition frequency between the two levels $|g\rangle$ and $|e\rangle$ of the atom. The creation (annihilation) operator of the cavity mode is denoted as a^\dagger (a), and the raising (lowering) operator of the atom is represented by σ_+ (σ_-).

In the absence of an additional driving field, we make a reasonable assumption that the total excitation of the system is unity [34, 36–39]. We denote the vacuum state (the single photon state) of the cavity as $|0\rangle$ ($|1\rangle$). In the basis states $|e, 0\rangle = |1, 0\rangle^T$ and $|g, 1\rangle = |0, 1\rangle^T$, where T stands for transpose, the effective Hamiltonian can be expressed as

$$H_{\text{eff}}^1 = \begin{pmatrix} \omega_a + \delta - \frac{i\gamma}{2} & g \\ g & \omega_a - \frac{i\kappa}{2} \end{pmatrix}, \quad (2)$$

where $\delta = \omega_e - \omega_a$ is the difference between the atomic transition frequency and the cavity frequency. The eigenvalues of the NH Hamiltonian (H_{eff}^1) are

$$E_{\pm} = \frac{1}{4} [2(2\omega_a + \delta) - i(\gamma + \kappa) \pm 2\Delta_E], \\ \Delta_E = \frac{i}{2} \sqrt{(\gamma - \kappa + 2i\delta)^2 - 16g^2}, \quad (3)$$

and the corresponding right eigenvectors are

$$|\phi_+\rangle = \frac{1}{S_+} [A_+, 4g]^T, \\ |\phi_-\rangle = \frac{1}{S_-} [A_-, 4g]^T, \quad (4)$$

where $A_{\pm} = 2\delta - i(\gamma - \kappa) \pm 2\Delta_E$ and $S_{\pm} = \sqrt{|A_{\pm}|^2 + |4g|^2}$, together with the left eigenvectors

$$\langle \widehat{\phi}_+ | = \frac{1}{S_+} [A_+, 4g], \\ \langle \widehat{\phi}_- | = \frac{1}{S_-} [A_-, 4g]. \quad (5)$$

The biorthogonal partners $\{|\widehat{\phi}_n\rangle\}$, $\{|\phi_m\rangle\}$ ($n, m = +, -$) are normalized to satisfy the biorthogonality and relations $\langle \widehat{\phi}_n | \phi_m \rangle = \delta_{nm}$, $\sum_n |\widehat{\phi}_n\rangle \langle \phi_n| = \sum_n |\phi_n\rangle \langle \widehat{\phi}_n| = 1$ [8, 40].

The difference $\Delta_E(\delta, g, \gamma, \kappa)$ between the eigenvalues (E_{\pm}) plays a pivotal role in determining the eigenenergy spectrum and the system dynamics. The analysis of Eq. (3) reveals that an EP occurs at $\delta = g = \gamma - \kappa = 0$ when $\Delta_E(\delta, g, \gamma, \kappa) = 0$. However, analyzing the relationship between all four parameters ($\delta, g, \gamma, \kappa$) and Δ_E simultaneously presents a significant challenge. Therefore, it is recommended to fix certain parameters and thoroughly investigate the correlation between the remaining parameters and Δ_E . This step is crucial for identifying EPs within the system.

Once the EPs are determined, the primary objective is to design a time evolution trajectory that encompasses the EPs in order to achieve asymmetric or symmetric Bell-state transfer. In this context, we provide several remarks regarding the design of the time evolution trajectory. (i) It is crucial to ensure that the eigenvectors $|\phi_+\rangle$ and $|\phi_-\rangle$ correspond to Bell states ($|1, 0\rangle \pm |0, 1\rangle$)/ $\sqrt{2}$ at both the beginning and end of the trajectory. To ensure the formation of Bell states, it is necessary to maintain $\delta_{t_i, t_f} = (\gamma - \kappa)_{t_i, t_f} = 0$ [where t_i (t_f) represents the initial (final) time], thereby $|\phi_+(t_i, t_f)\rangle$ and $|\phi_-(t_i, t_f)\rangle$ becoming Bell states can be satisfied. (ii) Both the real and imaginary components of the time evolution trajectory should be carefully designed to encircle or closely approach the EP. An improper trajectory design will give rise to significant nonadiabatic transitions, which may disrupt the intended state transfer during the system evolution. The subsequent sections will be dedicated to the exploration of appropriate time evolution trajectories for achieving symmetric and asymmetric Bell-state transfers.

III. SYMMETRIC BELL-STATE TRANSFER

Section II has demonstrated that the imaginary component $\text{Im}[\Delta_E(\delta, g, \gamma, \kappa)]$ has a detrimental effect on the symmetric state transfer, potentially leading to nonadiabatic transitions in the system dynamics [13–15]. To achieve efficient symmetric Bell-state transfers, one can eliminate $\text{Im}[\Delta_E(\delta, g, \gamma, \kappa)]$ by setting $\delta = 0$, and ensuring $16g^2 > (\gamma - \kappa)^2$. Furthermore, for the sake of discussion, we assume $\kappa = \alpha\gamma$ and scale all parameters with respect to the cavity frequency ω_a in the subsequent analysis.

Based on the aforementioned settings, we can investigate the intricate correlation between the energy difference and the remaining two parameters (g, γ) in a three-dimensional context. In order to gain an intuitive understanding of the energy variation within the system, in Fig. 1, we illustrate the eigenenergy spectrum E_{\pm} in the parameter space (g, γ). From Fig. 1(a), it is evident that the real parts of E_+ and E_- intersect with the plane defined by $E = 1$, their imaginary counterparts intersect

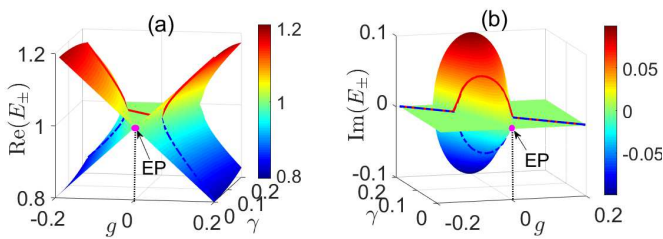


FIG. 1: The eigenenergy spectrum $E_{\pm}(g, \gamma)$ and the system's time-evolution trajectory $E_{\pm}[g(t), \gamma(t)]$ for symmetric Bell-state transfer. (a) the real part and (b) the imaginary part of $E_{\pm}(g, \gamma)$ and $E_{\pm}[g(t), \gamma(t)]$. The red (blue) Riemann surface corresponds to $E_{+}(g, \gamma)$ [$E_{-}(g, \gamma)$], and the solid red (dashed blue) line represents $E_{+}[g(t), \gamma(t)]$ [$E_{-}[g(t), \gamma(t)]$], respectively. The pink point is an EP. The other parameters are chosen as $g_0 = 0.01$, $G_0 = \Gamma_0 = 0.2$, $\alpha = -1$, and $\omega = \pi$.

with another plane characterized by $E = 0$. The intersection point of these two planes within the parameter space (g, γ) corresponds to a pink point at coordinates $(0, 0)$, which represents an EP. Consequently, by steering our system's evolution trajectory around or in close proximity to this EP, we can achieve a symmetric transfer of Bell states as desired.

A symmetric Bell-state transfer can be realized through the careful selection of the parameter trajectory

$$g(t) = g_0 + G_0 \cos(\omega t), \gamma(t) = \Gamma_0 \sin^2(\omega t), \quad (6)$$

where g_0 , G_0 , Γ_0 , and ω are real constants. According to Eq. (6), the NH Hamiltonian $H_{eff}^1(t)$ exhibits periodic variations with respect to time t , having a period of $T = \pi/\omega$. Figure 1 also illustrates the time-evolution trajectories, where the solid red line represents $E_{+}[g(t), \gamma(t)]$ and the dashed blue line corresponds to $E_{-}[g(t), \gamma(t)]$. It can be observed that both trajectories orbit in the vicinity of the pink EP, in accordance with our assumptions.

To evaluate the validity of the symmetric Bell-state transfer, we investigate the dynamics of the system. The fidelity of the right eigenstate $|\phi_m(t)\rangle$ ($m=+, -$) is determined by the relation $F_m = |\langle \widehat{\phi}_m(t) | \Psi(t) \rangle|^2$, where $|\Psi(t)\rangle$ represents the evolving state of the system at time t . Assuming that the system is initially prepared in one of its right eigenstates, i.e., $|\Psi(0)\rangle = |\phi_{\pm}(0)\rangle = (|e, 0\rangle \pm |g, 1\rangle)/\sqrt{2}$, we numerically integrate Schrödinger's equation to obtain the evolving state $|\Psi(t)\rangle$. The instantaneous left eigenvector $\langle \widehat{\phi}_m(t) |$ can be calculated by substituting parameters into Eqs. (5) and (6). The results of these calculations for different encircling directions and initialized states are illustrated in Fig. 2. Figures 2(a)-(d) demonstrate complete Bell-state transfers (achieving maximal transfer fidelity 1 by employing sufficiently slow trajectories), where $|\phi_{-}(t)\rangle \leftrightarrow |\phi_{+}(t)\rangle$ are exchanged after one period $T = \pi/\omega$, irrespective of encircling direction. The state evolution in this context demonstrates exclusive adiabatic characteristics, facilitating the implementation of asymmetric Bell-state switching.

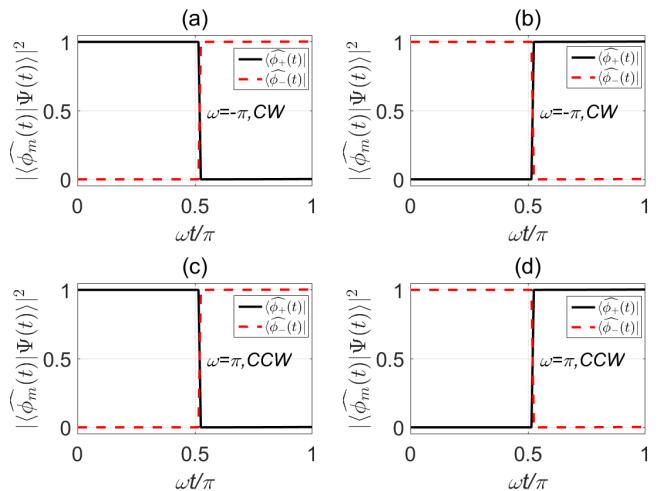


FIG. 2: The time evolution of the fidelity $F_m = |\langle \widehat{\phi}_m(t) | \Psi(t) \rangle|^2$ for the time-dependent right eigenstate $|\phi_m(t)\rangle$ ($m = +, -$). The initialized state in (a) and (c) [$|\phi_{+}(0)\rangle$] [$|\phi_{-}(0)\rangle$] is chosen as $|\Psi(0)\rangle = |\phi_{+}(0)\rangle$ [$|\phi_{-}(0)\rangle$]. The direction of trajectory in (a)-(b) is clockwise (CW) and in (c)-(d) is counterclockwise (CCW). The other parameters are chosen as $g_0 = 0.01$, $G_0 = \Gamma_0 = 0.2$, and $\alpha = -1$. The state dynamics exhibits a purely adiabatic character, enabling one to implement a symmetric Bell-state switch.

IV. ASYMMETRIC BELL-STATE TRANSFER

A. Asymmetric Bell-state transfer under time-modulated dissipations

The successful transfer of asymmetric or chiral Bell states relies on appropriately enhancing the weighting assigned to the imaginary component of the energy difference. Consequently, we proceed by fixing the value of g and exploring the relationship between the energy difference and the parameters (δ, γ) . We also present a graphical representation of the eigenenergy spectrum E_{\pm} in the parameter space (δ, γ) as depicted in Fig. 3. Figures 3(a) and (b) illustrate three-dimensional variations of the real part and the imaginary part respectively, while Fig. 3(c) provides an overhead view focusing on the real part of the energy spectrum. Figure 3(c) shows that both $E_{+}(\gamma, \delta)$ and $E_{-}(\gamma, \delta)$ converge along an L-shaped curve corresponding to $E = 1$. Furthermore, Fig. 3(b) demonstrates the convergence of both imaginary components of $E_{+}(\gamma, \delta)$ and $E_{-}(\gamma, \delta)$ at point $(0, 0)$. Comparison of Figs. 3(b) and (c) reveals the absence of EP under current parameter settings, as evidenced by the lack of coincidence between the L-shaped curve and point $(0, 0)$. Here, an approximate EP (AEP) is indicated by the pink point.

According to the conventional notion, the presence of EPs is deemed a prerequisite for the viability of the scheme, suggesting that chiral transformations are unattainable in their absence. However, it is intriguing

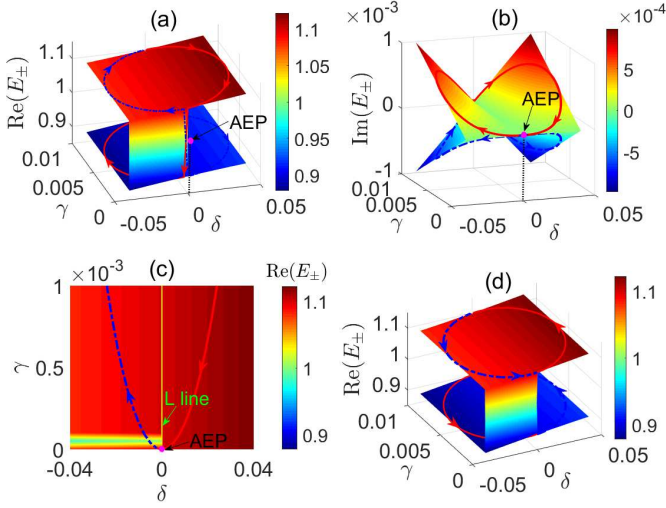


FIG. 3: The eigenenergy spectrum $E_{\pm}(\gamma, \delta)$ and the system's time-evolution trajectory $E_{\pm}[\gamma(t), \delta(t)]$ for an asymmetric Bell-state transfer. The real parts of the eigenenergy spectrum are presented in (a), (c), and (d), while the imaginary parts are shown in (b). Figure (c) provides an overhead view of figure (a) with $\gamma \subset (0, 0.001)$, where the red surface represents $E_{+}(\gamma, \delta)$ and the blue surface represents $E_{-}(\gamma, \delta)$. The pink point (0,0) in the parameter space (γ, δ) is an AEP. The solid red and dashed blue lines represent $E_{+}[\gamma(t), \delta(t)]$ and $E_{-}[\gamma(t), \delta(t)]$, and the orbiting trajectory in (a)-(c) [(d)] proceeds clockwise (counterclockwise), respectively. The other parameters are chosen as $g_0 = 0.1$, $\Delta_0 = 0.04$, $\Gamma_0 = 0.1$, and $\alpha = -1$.

to unveil that even when the system evolves around an AEP, a significant chiral transition still endures. This feasibility stems from the Riemann topology of the system spectrum induced by AEP and a specific selection of encircling trajectory within the parameter space. An asymmetric Bell-state transfer can be attained through a carefully selected parameter trajectory

$$\delta(t) = \Delta_0 \sin(\omega t), \gamma(t) = \Gamma_0 \sin^2\left(\frac{\omega t}{2}\right), \quad (7)$$

where Δ_0, Γ_0 , and $\omega \in \mathbf{R}$ are constants, the period of the trajectory is $T = 2\pi/\omega$. The time-evolution trajectories $E_{\pm}[\gamma(t), \delta(t)]$ are depicted in Fig 3. The orbiting trajectory proceeds in a counterclockwise (CCW) or clockwise (CW) direction for positive angular frequencies $\omega > 0$ or negative angular frequencies $\omega < 0$, respectively.

In Fig. 4, we present the temporal evolution of the fidelity for the right eigenstate $|\phi_m(t)\rangle$ ($m = +, -$) under different initial states and encircling directions. As illustrated in Figs. 4(a) and (b), the right eigenstates (Bell states) return to their original configurations after completing a dynamical cycle with a CW encircling direction. However, as shown in Figs. 4(c) and (d), the Bell states undergo an exchange after completing a dynamical cycle with a CCW encircling direction. The state dynamics exhibits a distinct chiral character, facilitating the implementation of a symmetric Bell-state switch.

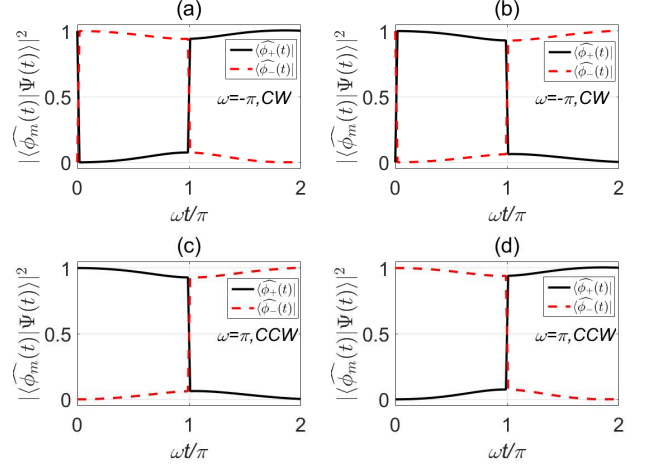


FIG. 4: The time evolution of the fidelity $F_m = |\langle \widehat{\phi}_m(t) | \Psi(t) \rangle|^2$ for the time-dependent right eigenstate $|\phi_m(t)\rangle$ ($m = +, -$). The initialized state in (a) and (c) [(b) and (d)] is chosen as $|\Psi(0)\rangle = |\phi_+(0)\rangle$ ($|\phi_-(0)\rangle$). The selected trajectories in (a)-(b) exhibit a clockwise (CW) encircling, while those in (c)-(d) demonstrate a counterclockwise (CCW) encircling. Other parameters are set as follows: $g_0 = 0.1$, $\Delta_0 = 0.04$, $\Gamma_0 = 0.1$, and $\alpha = -1$. The state dynamics exhibits a chiral in nature, thus, enabling one to implement an asymmetric Bell-state switch.

B. Asymmetric Bell-state transfer under time-independent dissipations

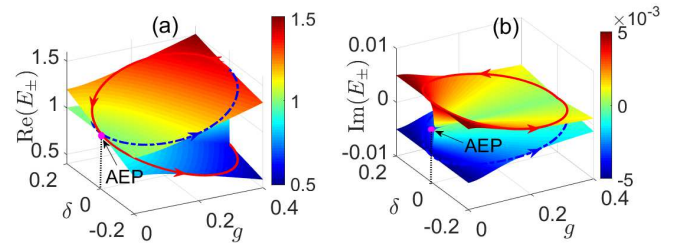


FIG. 5: The eigenenergy spectrum $E_{\pm}(g, \delta)$ and the system's time-evolution trajectory $E_{\pm}[g(t), \delta(t)]$ for a dissipative system with time-independent dissipation. (a) the real part and (b) the imaginary part of $E_{\pm}(g, \gamma)$ and $E_{\pm}[g(t), \gamma(t)]$. The red (blue) Riemann surface corresponds to $E_{+}(g, \gamma)$ [$E_{-}(g, \gamma)$], and the solid red (dashed blue) line represents $E_{+}(g, \gamma)$ ($E_{-}(g, \gamma)$), respectively. The pink point is an AEP. Other parameters are set as follows: $g_0 = G_0 = \Delta_0 = 0.2$, $\gamma_0 = 0.1$, $\alpha = -1$, and $\omega = \pi$.

We have successfully demonstrated the remarkable achievement of chiral Bell-state transfer through modulating time-dependent dissipative parameters. However, it is important to acknowledge that managing noise parameters can present challenges in certain systems or experiments. From an experimental perspective, we propose an alternative approach for achieving chiral Bell-state transfer by utilizing time-independent dissipative

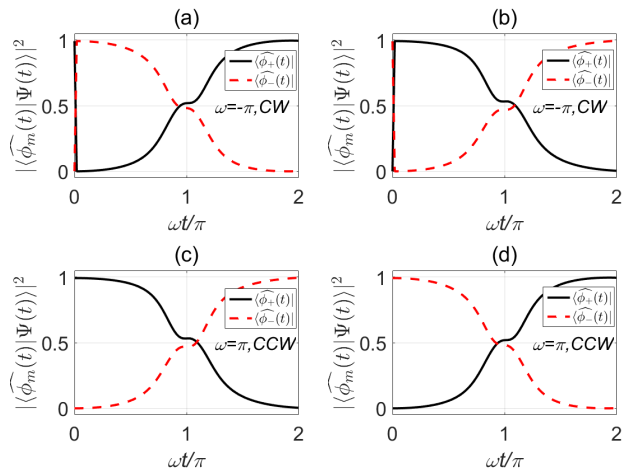


FIG. 6: The time evolution of the fidelity $F_m = |\langle \widehat{\phi}_m(t) | \Psi(t) \rangle|^2$ is examined for the time-dependent right eigenstate $|\phi_m(t)\rangle$ ($m = +, -$). The initial state in (a) and (c) [(b) and (d)] is selected as $|\Psi(0)\rangle = |\phi_+(0)\rangle$ ($|\phi_-(0)\rangle$). The chosen trajectory in (a)-(b) exhibits a CW encircling, while that in (c)-(d) displays a CCW encircling. The parameters are set as follows: $g_0 = G_0 = \Delta_0 = 0.2$, $\gamma_0 = 0.1$, and $\alpha = -1$.

parameters. Furthermore, we provide the eigenenergy spectrum E_{\pm} in the parameter space (g, δ) as shown in Fig 5. Figure 5(a) demonstrates the convergence of the real parts of $E_{\pm}(g, \delta)$ at point $(0,0)$, while Fig 5(b) showcases the separation between the imaginary parts of $E_{\pm}(g, \delta)$ at point $(0,0)$. Hence, under current parameter configuration, the system does not manifest any EP; instead, it exhibits a distinctive pink AEP.

The achievement of asymmetric Bell-state transfer can be realized by carefully selecting the parameter trajectory as follows:

$$\gamma(t) = \gamma_0, g(t) = g_0 + G_0 \cos(\omega t), \delta(t) = \Delta_0 \sin(\omega t), \quad (8)$$

where $g_0, G_0, \gamma_0, \Delta_0$, and $\omega, \in \mathbf{R}$ are constants, and the period of the trajectory is $T = 2\pi/\omega$. The time-evolution trajectories of $E_{\pm}(t)$ are also depicted in Fig 6. It can be observed that the trajectories of $E_{\pm}[g(t), \gamma(t)]$ encircle around the AEP. We also present the temporal evolution of the fidelity for the right eigenstate $|\phi_m(t)\rangle$ ($m = +, -$) under different initial states and encircling directions in Fig. 6. The state dynamics also exhibits a distinct chiral character, facilitating the implementation of a symmetric Bell-state switch.

V. CONCLUSION

We have theoretically demonstrated both symmetric and asymmetric Bell-state transfers in a J-C model

that incorporates atomic spontaneous emission and cavity decay. In the case of symmetric Bell-state transfer, we have effectively mitigated the impact of nonadiabatic transitions induced by the imaginary component of the eigenenergy spectrum through appropriate parameter settings. Thereby, we have achieved an efficient transfer by selecting a trajectory that dynamically encircles an EP. The proposed procedure enables a long-desired symmetric switch, wherein the Bell states are dynamically exchanged irrespective of the encircling direction. Furthermore, we have demonstrated chiral dynamics in the dissipative J-C model without a strict dependence on exceptional points (EP). Specifically, we have realized asymmetric Bell-state transfers even in the absence of EP while dynamically orbiting around an approximate exceptional point (AEP), where the final state is determined by trajectory orientation. Lastly, we have proposed an alternative approach to achieve chiral Bell-state transfers by utilizing time-independent dissipative parameters.

The presented results have potential applications beyond the Bell-state transfer through controlled dissipation, such as the transfer of multi-mode (hybrid) entangled states (e.g., GHZ state). Furthermore, our findings indicate that chiral dynamics can be achieved in NH systems without strict EP conditions, allowing for asymmetric state transfer while dynamically orbiting an AEP. This result has immediate implications for reducing parameter control complexity and experimental difficulties in NH systems with multiple types of dissipation. Hence, our work demonstrates a novel approach to manipulate entangled states with both symmetric and asymmetric characteristics using dissipation engineering, which is highly effective and reliable for quantum-state engineering in non-Hermitian systems.

ACKNOWLEDGEMENT

This work was supported by National Natural Science Foundation of China (NSFC) (Grants Nos. 12264040, 12374333, 12204311 and U21A20436), Jiangxi Natural Science Foundation (Grant Nos. 20232BCJ23022, 20224BAB201027, 20224BAB211025 and 20212BAB211018), Innovation Program for Quantum Science and Technology (Grant No. 2021ZD0301705) and the Jiangxi Province Key Laboratory of Applied Optical Technology (Grant No. 2024SSY03051).

[1] L. Feng, R. El-Ganainy and L. Ge, “Non-Hermitian photonics based on parity-time symmetry,” Nat. Photon. **11**,

- [2] Ş. Özdemir, S. Rotter, F. Nori, and L. Yang, “Parity-time symmetry and exceptional points in photonics,” *Nat. Mater.* **18**, 783 (2019).
- [3] W. D. Heiss, “Repulsion of resonance states and exceptional points,” *Phys. Rev. E* **61**, 929 (2000).
- [4] H. Cartarius, J. Main, and G. Wunner, “Exceptional points in atomic spectra,” *Phys. Rev. Lett.* **99**, 173003 (2007).
- [5] B. Peng, S. K. Özdemir, F. Lei, F. Monifi, M. Gianfreda, G. L. Long, S. Fan, F. Nori, C. M. Bender, and L. Yang, “Parity-timesymmetric whispering-gallery microcavities,” *Nat. Phys.* **10**, 394 (2014).
- [6] T. Kato, “*Perturbation Theory for Linear Operators*,” *Classics in Mathematics* (Springer, Berlin, 1995).
- [7] Y. Ashida, Z. Gong, and M. Ueda, “Non-Hermitian physics,” *Adv. Phys.* **69**, 249 (2020).
- [8] Q. C. Wu, J. L. Zhao, Y. L. Fang, Y. Zhang, D. X. Chen, C. P. Yang and F. Nori, “Extension of Noether’s theorem in PT-symmetry systems and its experimental demonstration in an optical setup,” *Sci. China-Phys. Mech. Astron.* **66**(4), 240312 (2023).
- [9] H. Hodaei, A. U. Hassan, S. Wittek, H. Garcia-Gracia, R. El-Ganainy, D. N. Christodoulides, and M. Khajavikhan, “Enhanced sensitivity at higher-order exceptional points,” *Nature* **548**, 187 (2017).
- [10] Z. Lin, H. Ramezani, T. Eichelkraut, T. Kottos, H. Cao, and D. N. Christodoulides, “Unidirectional invisibility induced by PT-symmetric periodic structures,” *Phys. Rev. Lett.* **106**, 213901 (2011).
- [11] A. Guo, G. J. Salamo, D. Duchesne, R. Morandotti, M. Volatier-Ravat, V. Aimez, G. A. Siviloglou, and D. N. Christodoulides, “Observation of PT-symmetry breaking in complex optical potentials,” *Phys. Rev. Lett.* **103**, 093902 (2009).
- [12] E. J. Bergholtz, J. C. Budich, and F. K. Kunst, “Exceptional topology of non-Hermitian systems,” *Rev. Mod. Phys.* **93**, 015005 (2021).
- [13] C. Guria, Q. Zhong, Ş. K. Özdemir, Y. S. S. Patil, R. El-Ganainy, and J. G. Emmet Harris, “Resolving the topology of encircling multiple exceptional points,” *Nat. Commun.* **15**, 1369 (2024).
- [14] I. I. Arkhipov, A. Miranowicz, F. Minganti, Ş. Özdemir, and F. Nori, “Restoring adiabatic state transfer in time-modulated non-hermitian systems,” *Phys. Rev. Lett.* **133**, 113802, (2024)
- [15] Q. C. Wu, J. L. Zhao, Y. H. Zhou, B. L. Ye, Y. L. Fang, Y. H. Kang, Q. P. Su, Z. W., Zhou and C. P. Yang, “Shortcuts to adiabatic state transfer in time-modulated two-level non-Hermitian systems,” *arXiv e-prints*, arXiv: **2411**, 00428 (2024).
- [16] S. Khandelwal, W. J. Chen, K. W. Murch, and G. Haack, “Chiral Bell-State Transfer via Dissipative Liouvillian Dynamics,” *Phys. Rev. Lett.* **133**, 070403 (2024).
- [17] M. V. Berry, “Optical polarization evolution near a non-Hermitian degeneracy,” *J. Opt. A* **13**, 115701 (2011).
- [18] H. Xu, D. Mason, Luyao Jiang, and J. G. E. Harris, “Topological energy transfer in an optomechanical system with exceptional points,” *Nature (London)* **537**, 80 (2016).
- [19] A. Li, J. Dong, J. Wang, Z. Cheng, J. S. Ho, D. Zhang, et al., “Hamiltonian hopping for efficient chiral mode switching in encircling exceptional points,” *Phys. Rev. Lett.* **125**(18), 187403 (2020).
- [20] J. Feilhauer, A. Schumer, J. Doppler, A. A. Mailybaev, J. Böhm, U. Kuhl, N. Moiseyev, and S. Rotter, “Encircling exceptional points as a non-Hermitian extension of rapid adiabatic passage,” *Phys. Rev. A* **102**, 040201 (2020).
- [21] M. S. Ergoktas, S. Soleymani, N. Kakenov, K. Wang, T. B. Smith, G. Bakan, S. Balci, A. Principi, K. S. Novoselov, S. K. Ozdemir, and C. Kocabas, “Topological engineering of terahertz light using electrically tunable exceptional point singularities,” *Science* **376**, 184 (2022).
- [22] I. I. Arkhipov, A. Miranowicz, F. Minganti, Ş. Özdemir, and F. Nori, “Dynamically crossing diabolic points while encircling exceptional curves: A programmable symmetricasymmetric multimode switch,” *Nat. Commun.* **14**, 2076 (2023).
- [23] Z. Tang, T. Chen, and X. Zhang, “Highly efficient transfer of quantum state and robust generation of entanglement state around exceptional lines,” *Laser Photonics Rev.* 2300794 (2023).
- [24] A. U. Hassan, G. L. Galmiche, G. Harari and P. LiKamWa, “Chiral state conversion without encircling an exceptional point,” *Phys. Rev. A* **96**, 052129 (2017).
- [25] A. U. Hassan, B. Zhen, M. Soljačić, M. Khajavikhan, and D. N. Christodoulides, “Dynamically encircling exceptional points: Exact evolution and polarization state conversion,” *Phys. Rev. Lett.* **118**, 093002 (2017).
- [26] X. L. Zhang, T. Jiang, and C. T. Chan, “Dynamically encircling an exceptional point in anti-parity-time symmetric systems: Asymmetric mode switching for symmetrybroken modes,” *Light Sci. Appl.* **8**, 88 (2019).
- [27] H. Nasari, G. L. Galmiche, H. E. L. Aviles, A. Schumer, A. U. Hassan, Q. Zhong, S. Rotter, P. LiKamWa, D. N. Christodoulides and M. Khajavikhan, “Observation of chiral state transfer without encircling an exceptional point,” *Nature* **605**, 256 (2022).
- [28] F. Verstraete, M. M. Wolf and J. I. Cirac, “Quantum computation and quantum-state engineering driven by dissipation,” *Nat. Phys.* **5**(9), 633 (2009).
- [29] Q. C. Wu, Y. H. Zhou, B. L. Ye, T. Liu and C. P. Yang, “Nonadiabatic quantum state engineering by time-dependent decoherence-free subspaces in open quantum systems,” *New J. Phys.* **23**, 113005 (2021).
- [30] J. Zou, S. Zhang, and Y. Tserkovnyak, “Bell-state generation for spin qubits via dissipative coupling,” *Phys. Rev. B* **106**, 180406 (2022).
- [31] N. Schine, A. W. Young, W. J. Eckner, M. J. Martin and A. M. Kaufman, “Long-lived Bell states in an array of optical clock qubits,” *Nat. Phys.* **18**, 1067-1073 (2022).
- [32] B. W. Shore and P. L. Knight, “The jaynes-cummings model,” *J. Mod. Optic.* **40**, 1195, (1993).
- [33] L. S. Bishop, E. Ginossar and S. M. Girvin, “Response of the Strongly Driven Jaynes-Cummings Oscillator,” *Phys. Rev. Lett.* **105**, 100505 (2010).
- [34] Y. H. Zhou, H. Z. Shen, X. Y. Zhang, and X. X. Yi, “Zero eigenvalues of a photon blockade induced by a non-Hermitian Hamiltonian with a gain cavity,” *Phys. Rev. A* **97**, 043819 (2018).
- [35] C. Liu, J. F. Huang, “Quantum phase transition of the Jaynes-Cummings model,” *Sci. China-Phys. Mech. Astron.* **67**(1), 240312 (2024).
- [36] J. Li, R. Yu, and Y. Wu, “Proposal for enhanced photon blockade in parity-time-symmetric coupled microcavities,” *Phys. Rev. A* **92**, 053837 (2015).

- [37] L. Feng, Z. J. Wong, R.-M. Ma, Y. Wang, and X. Zhang, “Single-mode laser by parity-time symmetry breaking,” *Science* **346**, 972 (2014).
- [38] W. Chen, Ş. Özdemir, G. Zhao, J. Wiersig, and L. Yang, “Exceptional points enhance sensing in an optical microcavity,” *Nature (London)* **548**, 192 (2017).
- [39] I. I. Arkhipov, A. Miranowicz, F. Nori, Ş. K. Özdemir, and F. Minganti, “Fully solvable finite simplex lattices with open boundaries in arbitrary dimensions,” *Phys. Rev. Res.* **5**, 043092 (2023).
- [40] D. C. Brody, “Biorthogonal quantum mechanics,” *J. Phys. A-Math. Theor.* **47**, 035305 (2013).